Theor Chem Acc (2012) 131:1099
DOI 10.1007/s00214-012-1099-9

REGULAR ARTICLE

Potential of bifluorenylidene derivatives as nonfullerene small-molecule acceptor for heterojunction organic photovoltaics: a density functional theory study

Guang-Yan Sun · Hai-Bin Li · Yun Geng · Zhong-Min Su

Received: 2 October 2011 / Accepted: 20 January 2012 / Published online: 4 March 2012

Abstract To maximize the efficiency of heterojunction organic photovoltaics (HJOPVs), it is imperative to increase not only the open-circuit voltage (V_{OC}) but also the short-circuit current (I_{SC}). Therefore, it is desirable to find an organic acceptor material that possesses a higher lowest unoccupied molecular orbital (LUMO) level for higher V_{OC} and can absorb photons in the solar spectrum efficiently for larger I_{SC}. In this paper, in comparison with the typical donor poly(3-hexylthiophene) (P3HT) and acceptor [6,6]-phenyl-C_{61}-butyric acid ester ([60]PCBM), the geometries, electronic structures, absorption spectra, and transport properties of a series of organic compounds containing 9,9′-bifluorenylidene (9,9′**BF**) were systematically investigated using density functional and the semiclassical Marcus charge transfer theory calculation to evaluate their potential severing as acceptor. Our results indicate that the absorption spectra of 99′**BF** derivatives have better overlap with the solar spectrum than those of [60]PCBM, and higher LUMOs result in a significant enhancement of V_{OC} when they are used in HJOPVs with P3HT as donor materials. On the other hand, these compounds own higher electron carrier mobilities comparing with [60]PCBM. The study also demonstrates that the H-shaped compounds based on the 99′**BF** backbone possess good photophysical and charge transport properties, can be promising organic semiconductor for heterojunction photovoltaics.

Keywords 9,9′-Bifluorenylidene · Photoactive material · Electronic spectrum · Transport · Density functional theory

1 Introduction

Solar energy is one kind of the most promising energy that is abundant, clean, and renewable, and it is an ideal alternative to the traditional energy sources [1]. In the past decades, silicon-based inorganic solar cells have achieved great development, and many commercial products of the solar cells have been used in our daily life. However, there exist some disadvantages in the silicon-based solar cells at present, such as high cost, heavy weight, high environmental pollution, limited silicon sources and purification of silicon materials, and energy consumption in the production [2]. A number of new-generation organic solar cells (OSCs) are currently under investigation, including polymer bulk heterojunction solar cells and small-molecule solar cells, which are promising candidates for future applications, and have been extensively investigated in detail because of the tunability of their physical and chemical properties by rational sequential structural modification and the advantages of easy fabrication, low cost, light weight, and the possibility to fabricate flexible devices in comparison with traditional inorganic semiconductor photovoltaics [3–10]. Heterojunction organic photovoltaics (HJOPVs) are commonly composed of a photoactive blend film of a donor and acceptor sandwiched between a

Electronic supplementary material The online version of this article (doi:10.1007/s00214-012-1099-9) contains supplementary material, which is available to authorized users.

G.-Y. Sun · Z.-M. Su
Key Laboratory of Natural Resources of the Changbai Mountain & Functional Molecules (Yanbian University), Ministry of Education, Yanji 133002, Jilin, China

G.-Y. Sun · H.-B. Li · Y. Geng · Z.-M. Su (✉)
Institute of Functional Material Chemistry, Faculty of Chemistry, Northeast Normal University, Changchun 130024, Jilin, China
e-mail: zmsu@nenu.edu.cn

PEDOT: PSS-coated ITO-positive electrode and a low workfunction metal negative electrode. To guarantee high-efficiency HJOPVs devices, photoactive materials must be satisfied with several important conditions: (1) broad visible absorption, (2) higher charge carrier mobility, and (3) suitable electronic energy levels of both the donor and acceptor materials [11, 12]. In order to further improve the power conversion efficiency (PCE) of HJOPVs, much research work has been devoted to finding new donor materials aiming at broader absorption, lower bandgap, higher hole mobility, and suitable electronic energy levels, and some donor materials showing higher photovoltaic efficiency [13–17]. However, the research efforts devoted to the acceptors are much less than those on donors. Although some n-type conjugated polymers with stronger visible absorption have been applied as acceptors in the HJOPVs [18–20], the fullerene derivatives [6,6]-phenyl-C_{61}-butyric acid ester ([60]PCBM) and [6,6]-phenyl-C_{71}-butyric acid methyl ester ([70]PCBM) still dominate the acceptors in HJOPVs for their high efficiency.

It is well known that [60]PCBM and [70]PCBM are the most successful acceptor materials that have been used in HJOPVs [21–24]. Extensive researches and applications have been focused on them in the field of material sciences [8]. Among such studies, the development of fullerene-based polymer solar cells has attracted significant interest in recent years, because fullerenes have been recognized as excellent electron acceptors due to their unique π-electron system and excited state electronic properties [25–27]. However, there are some limitations in [60]PCBM as an acceptor material in HJOPVs: low charge mobility, weak absorption in the visible spectrum, and low open-circuit voltage (V_{OC}) (about 0.6 V) [28, 29]. The low absorption can be attributed to a high degree of symmetry, making the lowest-energy transitions formally dipole forbidden. The low V_{OC} is due to the extremely deep-lying lowest unoccupied molecular orbital (LUMO) levels of [60]PCBM [30]. Despite the wide use of these fullerene derivatives, the synthesis of new acceptor materials at energy levels is greatly significant from those of current fullerene derivatives, and wide versatility in terms of derivatization and functionalization of new acceptor materials is urgently required [9, 10, 31]. During the past few years, higher-order, multidimensional systems with novel architectures and sophisticated topologies have emerged as a consequence of increased versatility of semiconductors for HJOPVs [32, 33]. Recent representative new π-conjugated materials including star-shaped [34, 35], X-shaped [36], swivel cruciform [37, 38], spider-like [39], macrocyclic [40], and dendritic [41] greatly broaden the scope of molecular candidates for HJOPVs [42, 43].

Recently, Wudl and co-workers reported a new generation of H-shaped compounds based on the 9,9′-bifluorenylidene (99′**BF**) backbone [44]. The two fluorenyl-containing conjugated arms are bridged by a rigid C=C double bond that is different from the C–C single bond presented in the strain cruciform configuration. The free rotation of the two arms is forbidden, which allows efficient electronic coupling between the two fluorenyl-containing conjugated units. 99′**BF** derivatives with upshifted LUMO energy levels were developed, and HJOPVs based on poly(3-hexylthiophene) (P3HT) as donor and the new 99′**BF** derivatives as acceptor show high V_{OC} and improved photovoltaic efficiency [44]. However, the comprehensive studied on the electronic structures and spectral and transport properties of 99′**BF** derivatives as acceptor for HJOPVs in theory is sparse.

In the present work, we carried out density functional theory (DFT) calculations on the electronic structures and spectral properties of a series of 99′**BF** derivatives. Their molecular structures are shown in Fig. 1. The transport properties were investigated by combining DFT calculations with the semiclassical Marcus charge transfer theory, which are proved to give good estimates of the carrier mobility values [45–47]. It is a fundamental and important investigation for the synthetic study and reasonable design of high-performance acceptor materials of HJOPVs.

2 Theoretical methodology and computational methods

To describe the charge transport properties of 99′**BF** derivatives, we employed the incoherent hopping model

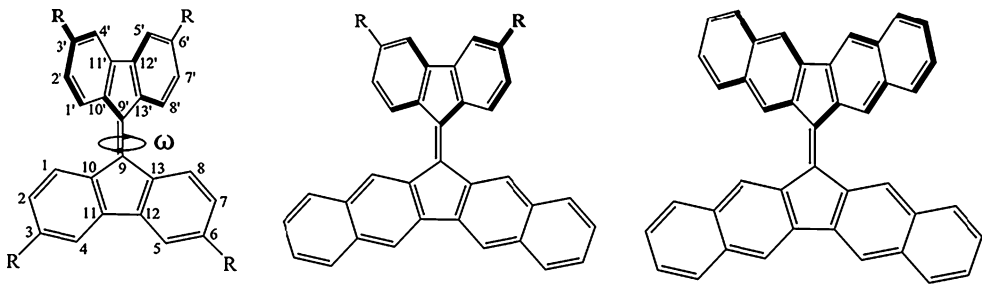

1a R=H
1b R=OMe

2a R=H
2b R=OMe

3

Fig. 1 Chemical structures and bond designations of the investigated systems

[45, 48–50] in which charge can transfer only between neighboring molecules. Each hopping step has been considered as a nonadiabatic electron transfer reaction involving a self-exchange charge from a charged molecule to an adjacent neutral one. The rate of intermolecular charge transfer (k) can be estimated from the semiclassical Marcus theory [46, 47] given by:

$$k = V^2 \sqrt{\frac{\pi}{\hbar^2 k_B T \lambda}} \exp\left(-\frac{\lambda}{4 k_B T}\right) \quad (1)$$

where T is the absolute temperature, V is the transfer integral, λ is the reorganization energy, and $\hbar$ and k_B are the Planck and Boltzmann constants, respectively. Therefore, the large transfer rate can be attributed to the maximal transfer integral and the minimal reorganization energy. The drift mobility of hopping μ can be evaluated from the Einstein relation:

$$\mu = \frac{e}{k_B T} D \quad (2)$$

where e is the electronic charge and D is the diffusion coefficient, which is related to the charge-transfer rate k as summing over all possible hops. The diffusion coefficient can be approximately evaluated as [51–53]:

$$D = \frac{1}{2n} \sum_i r^2 k_i P_i \quad (3)$$

where $n = 3$ is the dimensionality, k_i is the hopping rate due to charge carrier to the ith neighbor, and i represents a specific hopping pathway with r being the hopping distance. Here, we assume that the charge hopping occurs only between nearest neighbor molecules. P_i is the relative probability for charge carrier to a particular ith neighbor:

$$P_i = k_i / \sum_i k_i \quad (4)$$

Using Eqs. 1–4, the carrier mobility can be calculated. However, what is still lacking is how to obtain the intermolecular transfer integral V and reorganization energy λ. The transfer integral characterizes the strength of electronic coupling between the two adjacent molecules. The charge-transfer integral can be obtained either by Koopmans' theorem (indirect method) [54] or by the direct dimmer Hamiltonian evaluation method [52, 55, 56]. In the former case, Brédas et al. cautioned recently that when the dimer is not cofacial, the site energy correction should be taken into account due to the crystal environment [57]. The charge-transfer integrals for electron transport could be obtained from the direct method and can be written as:

$$V = \left\langle \Phi_{\mathrm{LUMO}}^{0,\mathrm{site1}} | F | \Phi_{\mathrm{LUMO}}^{0,\mathrm{site2}} \right\rangle \quad (5)$$

where $\Phi_{\mathrm{LUMO}}^{0,\mathrm{site1}}$ and $\Phi_{\mathrm{LUMO}}^{0,\mathrm{site2}}$ represent the LUMO of isolated molecules 1 and 2, respectively, and F is the Fock operator for the dimer with a density matrix from the noninteracting dimer of $F = SC\varepsilon C^{-1}$, where S is the intermolecular overlap matrix and C and ε are the molecular orbital coefficients and energies from one-step diagonalization without iteration.

Generally, reorganization energy is composed of both the internal reorganization energy (λ_i) and the external reorganization energy (λ_e) [58, 59]. The external reorganization energy is induced by the electronic and nuclear slow variations in solvent polarization of the surrounding medium. In this article, the external reorganization energy is neglected [60]. As a result, the internal contribution becomes the dominant factor. The inner reorganization energy (λ_i) is caused by the change of the internal nuclear coordinates from the reactant A to the product B and vice versa (See in the Electronic Supplementary Information Figure S1). It can be evaluated as the sum of two relaxation energies according to the following formula:

$$\lambda_i = \lambda_0 + \lambda_1 = \left(E_B^A - E_A^A\right) + \left(E_A^B - E_B^B\right) \quad (6)$$

where E_B^B and E_B^A represent the neutral and ionic energy with the neutral geometry, and E_A^B and E_A^A represent the neutral and ionic energy with the ionic geometry.

All calculations were performed with the Gaussian 09 program package [61]. Geometric and electronic structures of the considered 99′**BF** derivatives as well as anionic and neutral states structures were investigated by B3LYP/6-31G(d) [62]. Full geometric optimizations without symmetry constraints were carried out. Vibrational frequencies were also evaluated to check that the anionic and neutral states are the potential energy minima. The transition energies of these 99′**BF** derivatives were calculated at the optimized ground-state geometries by TDDFT, B3LYP/6-31G(d). The charge-transfer integral calculations were performed by using the PW91PW91/6-31G** method. It has been demonstrated that this is an appropriate choice of functional for the DFT level [55, 63].

3 Results and discussion

3.1 Equilibrium geometries

A factor for understanding transport properties in organic π-conjugated molecules is to identify those structural factors which depend on molecular architecture. The optimized neutral geometric parameters of all the compounds by B3LYP/6-31G(d) are presented in Table S1 (in Supporting Information) along with the available X-ray

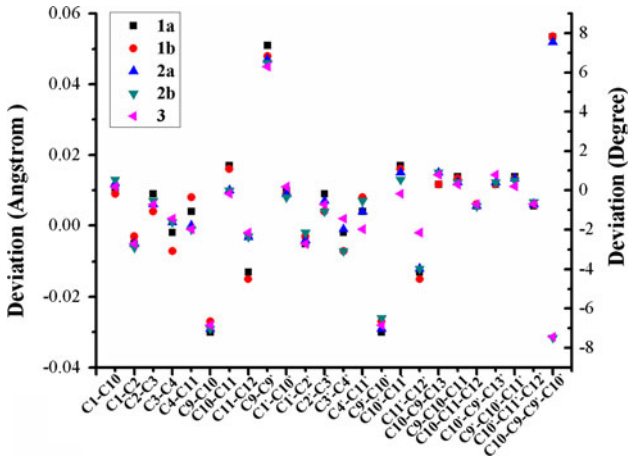

Fig. 2 Deviation values of the geometrical parameters differences between the neural and anion states for **1a**, **1b**, **2a**, **2b**, and **3**. (Due to structural symmetry of each compound, only half molecule was analyzed)

crystal diffraction data [44, 64]. The calculated results are found to be in good agreement with the experimental ones. This indicates that the adopted functional and basis sets are suitable to the studied systems. To further understand the effects of electron trapped in these molecules, we optimized the anion geometry. Calculated main changes of geometric parameters for anion and neutral states are listed in Fig. 2. The optimized structures for anion show smaller structural changes relative to the neutral. The main influences of the injection of one electron are focused on the change of C9=C9′ bond length and C10–C9–C9′–C10′ dihedral angle. Based on the small structural relaxation, we expect that these compounds would exhibit a relatively high structural stability versus the injection of one electron. Consequently, these compounds are good at electron holding, which extend the lifetime of charge separation states for efficient charge collection [65, 66].

3.2 Electronic structures and absorption spectra

Since the optoelectronic properties such as excitation energies and charge transport are closely related to the frontier molecular orbitals (FMOs) [67], so we show the FMOs of all compounds in Fig. 3. The HOMOs and LUMOs exhibit π and π^* orbital features, respectively, and both spread over the whole core. In general, a more delocalized LUMO would lead to easier electron transport by hopping. It can be seen from the distributions of LUMOs that studied systems will be favorable for electron transport. In addition, it can be seen from Fig. 3 that since methoxy group has some contributions to molecular orbitals, the energy levels of FMOs are effectively tuned. The V_{OC} of HJOPVs is determined by the difference between the LUMO energy of the 99′**BF** acceptors and the HOMO energy of the donors [11]. Thereby, the electronic energy levels of the 99′**BF** derivatives are very important for the application as acceptor in HJOPVs, especially for LUMO. Here, we show our results on the LUMO energy levels of 99′**BF** derivatives and [60]PCBM by B3LYP/6-31G(d) calculation (seen in Fig. 4). Compared with [60]PCBM, the LUMO energies of 99′**BF** derivatives are moved upward by at least 0.54 eV, which is favorable and may result in high V_{OC} when they are used as acceptors in HJOPVs. At the same time, it can be seen from Fig. 4 that the LUMO levels increase with introducing CH_3O– groups: (**1a**) (−2.50 eV) < (**1b**) (−2.01 eV), (**2a**) (−2.49 eV) < (**2b**) (−2.27 eV). So, there should be enough space for upshift of the LUMO energy level of new 99′**BF** derivatives acceptors to get higher V_{OC} and thus to improve PCE of the HJOPVs. However, to efficiently dissociate exciton present at interface between donor and acceptor, there should be enough driving force, namely the energy difference between the LUMO of donor and acceptor. Usually, the value of driving force is considered to be about 0.3 eV. As for nonfullenene acceptor **1b**, the driving force

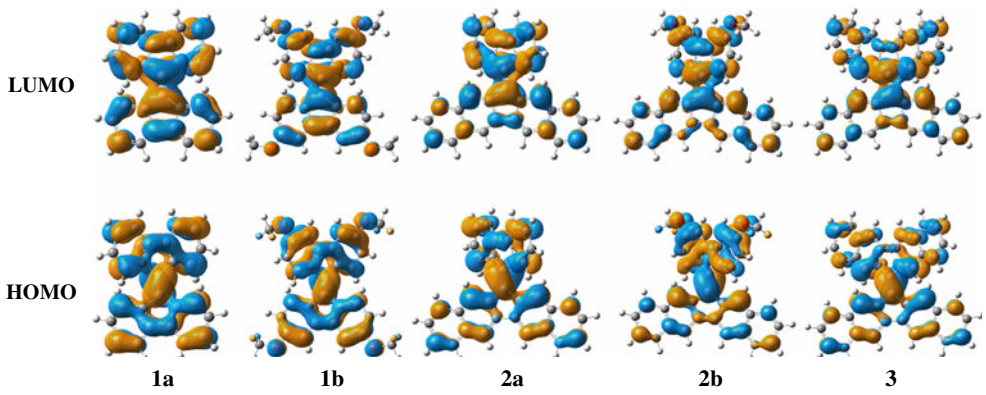

Fig. 3 Frontier molecular orbital diagrams for all compounds by B3LYP/6-31G(d) calculation

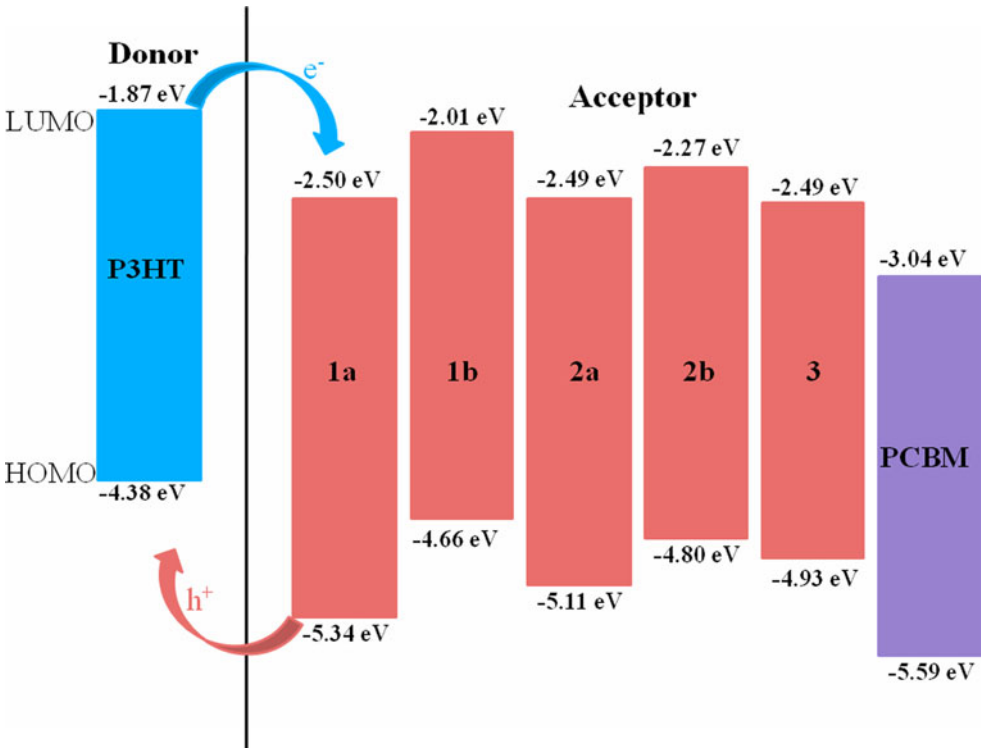

Fig. 4 Energy level diagrams of the investigated systems by B3LYP/6-31G(d) calculation

is less than this commonly used threshold, which could be the potential reason that Wudl and co-workers did not make great effort to prepare and optimize the OPVs devices based on **2a** [68].

Based on the structural analysis of compounds **1a–3**, absorption energies were calculated at optimized S_0 geometries using TD-DFT method to study their optical properties. DFT has been remarkably successful in providing a means for computing a variety of excitation energies with an accuracy which rivals that of the ab initio level methods, we tested the conventional DFT-based methods with different exchange–correlation functional on the excitation energies of **1a**. The results show that the adopted functional (B3LYP) is suitable to the studied systems (Figure S2. in Supporting Information). Furthermore, in order to investigate the influence of basis set, we employed five basis sets, that is, 6-31G(d), 6-31G(d,p), 6-31+G(d), 6-31+G(d,p), 6-31++G(d,p), and POL1 [69], to calculate the excitation energies of **1a** by using B3LYP functional. The data are depicted in Figure S2(b). The results suggest that the 6-31G(d) basis set is satisfactory for the calculation of excitation energies and can save computer times; thus, we employed it for all calculations. The absorption spectra were simulated with a Gaussian-type curve in vacuum for the studied compounds (shown in Fig. 5), and the full width at half-maximum value used for the simulated spectra was 3,000 cm^{-1}. The detailed information including excitation energies, oscillator strengths (*f*), dominant configurations, transition nature,

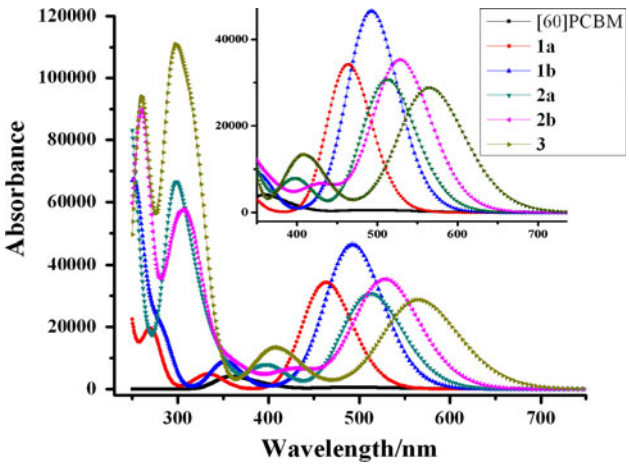

Fig. 5 Simulated absorption spectra for 99′**BF** derivatives and [60]PCBM at TDDFT B3LYP/6-31G(d) level. The value of the FWHM is 3,000 cm^{-1}

and experimental values of these compounds is listed in Table S2 of the Supporting Information.

The absorption properties are very important for photovoltaic materials. Figure 5 shows the UV–Vis absorption spectra of 99′**BF** derivatives along with [60]PCBM in vacuum for comparison. In the UV–visible region from 200 to 700 nm, the absorbance of 99′**BF** derivatives is much stronger than that of [60]PCBM (see inset of Fig. 5). Thus, 99′**BF** derivatives can be widely used instead of [60]PCBM as acceptor in the HJOPVs for enhancing the solar light harvest in the wavelength region**.** The main absorption

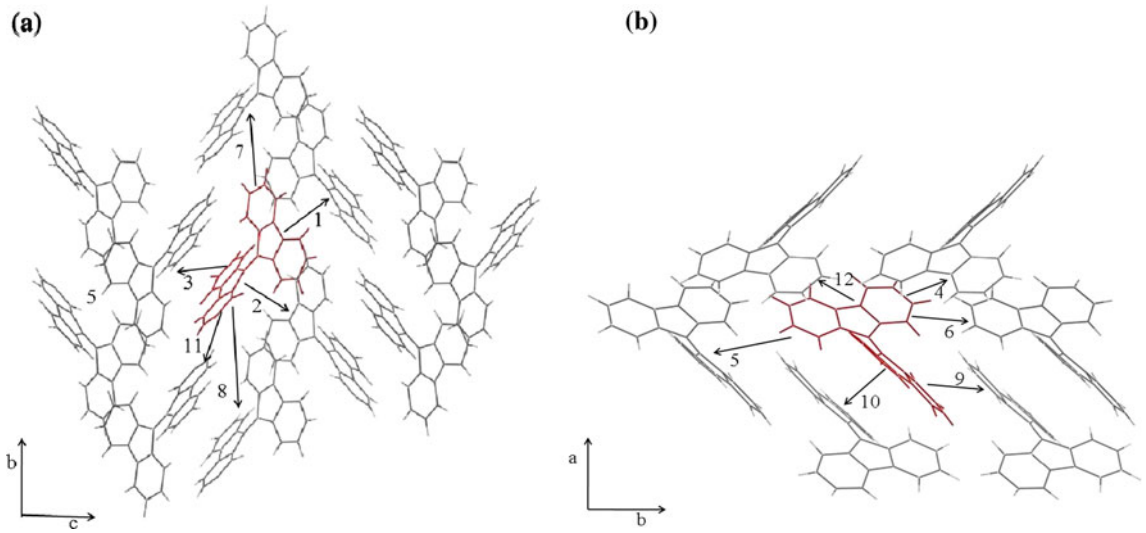

Fig. 6 Carrier transport pathways of **1a**. **a** In *bc* plane and **b** In *ab* plane

peaks all arise from the promotion of one electron between S_0 and S_1. The lowest $S_0 \rightarrow S_1$ electronic transitions for them originate from HOMO → LUMO transition, that is, $\pi \rightarrow \pi^*$ transition. However, methoxy group substitutions have great intensified on the intensity of absorption spectra in the visible and UV region, which are well in agreement with the analysis of the frontier molecular orbitals. We also found that the absorption of **3** with the largest absorption wavelength is shifted to longer wavelengths by approximately 90 nm compared with that of the parent compound **1a** because of the enhanced π-electron delocalization. In comparison with traditional acceptor materials of photovoltaic devices based on [60]PCBM, the absorption spectra of these compounds have a greater degree of overlap solar spectrum in the visible, which is very favorable on the development and application for the use as acceptor in HJOPVs.

3.3 Charge transport properties

In addition to the V_{OC} influencing the overall photovoltaic performance, the high short-circuit current (I_{SC}) and fill factor (FF), which are in close connection with charge mobility, are also crucial to improve its performance. As for the mobility, reorganization energy (λ) and transfer integrals (V) are the two key parameters affecting its magnitude.

The intramolecular reorganization energies of all compounds were evaluated from adiabatic potential energy surfaces based on B3LYP/6-31G(d) method. From the reorganization energies, we can find that the introduction of methoxy group induces larger λ_{ie} of **1b** (0.41 eV) and **2b** (0.33 eV) than that of **1a** (0.35 eV), **2a** (0.30 eV), and **3** (0.28 eV). This phenomenon is in good agreement with the discussion on geometric parameters. As a result, just from the λ_{ie} perspective, we can reasonably infer that the tendency of electron mobility may conform to the order of **3** > **2a** > **1a** > **2b** > **1b**. It should be noted that the λ_{ie} is just one of the key factors that influence the electron mobility of compounds and other factors such as parameter-electronic coupling (electron transfer integral) should be taken into account. In what follows, the electron transfer integrals of these compounds will be further discussed in detail.

To obtain rational transfer integrals (V), all of the possible hopping pathways (dimer) of **1a** and **2b** have been considered based on their crystal structures [44, 45]. The hopping pathways of **1a** and **2b** are shown in Figs. 6 and 7, respectively. Their corresponding dimer center of mass (CM) distances and transfer integrals are also presented in Tables 1 and 2. The value of V is mainly determined by the orbital interaction between the two adjacent molecules. Therefore, the orbital distributions and phase of the two adjacent molecules have significant influence on the transfer integral. The two contacting orbitals with the same phase display a large transfer integral. The intermolecular noncovalent bonds often impact V_e. For a hopping pathway, the Ve depends on the electron coupling between the LUMO and LUMO + 1. For example, the slipped and π-stacked arrangement of **1a** is observed. In the *bc* plane, we can find that there are two nearest neighbors for each molecule to form main charge hopping pathways. The larger electron transfer integrals for path 1 and 2 (46 meV) are ascribed to face-to-face π stacking of two adjacent half molecules with a close distance (about 6.6 Å). It is noted that other adjacent molecules are also described here, which are possessed of the smaller transfer integrals with large distances between the two molecular centers and less

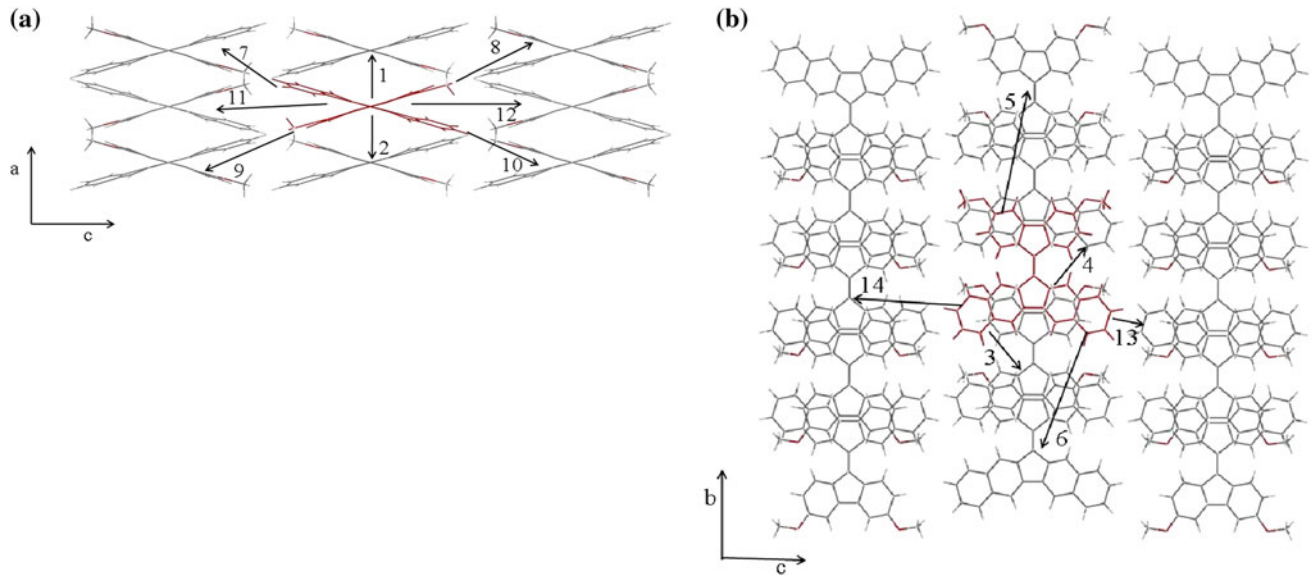

Fig. 7 Carrier transport pathways of **2b**. **a** In *ac* plane and **b** In *bc* plane

Table 1 Calculated electron transfer integrals (meV) and dimer CM distance (Å) of **1a**

Pathway	Dimer CM distance	$V_{Electron}$	Pathway	Dimer CM distance	$V_{Electron}$
1	6.646	46	7	9.715	9.38
2	6.646	46	8	9.715	9.38
3	6.935	24.5	9	10.237	−0.466
4	6.935	24.5	10	10.237	−0.466
5	8.991	−7.68	11	11.885	−0.583
6	8.991	−7.68	12	11.885	−0.583

Table 2 Calculated electron transfer integrals (meV) and dimer CM distance (Å) of **2b**

Pathway	Dimer CM distance	$V_{Electron}$	Pathway	Dimer CM distance	$V_{Electron}$
1	7.236	−7.38	10	13.841	−1.23
2	7.236	−7.38	11	14.159	0.165
3	7.236	−0.046	12	14.159	0.165
4	7.236	−7.38	13	15.284	1.13
5	12.475	−0.046	14	15.284	1.13
6	12.475	1.13	15	17.722	0.00752
7	13.841	−1.23	16	17.722	0.00752
8	13.841	−1.23	17	17.722	0.00752
9	13.841	−1.23	18	17.722	0.00752

intermolecular overlap of orbitals for path 9–10 and path 11–12, while for **2b**, its crystal structure is slightly similar to **1a**'s, which has eighteen main charge transfer pathways assigned to the typical dimers (depicted in Fig. 7), and the transfer integrals are smaller owing to smaller orbital overlaps and weaker intermolecular interactions with the farther distance than **1a**'s.

Combining the parameters mentioned above with Eqs. 1, 2, we estimated the electron mobilities (μ) of 47×10^{-3} cm^2/V·s for **1a** and 2.13×10^{-3} cm^2/V·s for **2b**

based on all of the possible hopping pathways shown in Figs. 6 and 7, respectively. The electron mobility of **1a** and **2b** exceeds that of [60]PCBM (2.00×10^{-3} $cm^2/V{\cdot}s$) [70]. This proves that H-shaped compounds with strain and Hückel aromaticity based on 99′**BF** backbone have good energy level and spectral and electron transport properties. However, 99′**BF** derivatives can be acceptor materials for HJOPVs may be premature for air stability due to the lower electron affinities. For this problem, we believe that experimental chemists need to improve complexity of processing technology and active layer morphology of device, thus to improve the photovoltaic efficiency.

4 Conclusions

By employing density functional theory (DFT) and the semiclassical Marcus charge transfer theory, we systematically investigated the electronic structures and spectral and transport properties for low-bandgap conjugated organic compounds 99′**BF** derivatives as acceptor for HJOPVs in molecule scale. The results show that 9,9′**BF** derivatives have a significant enhancement of V_{OC} than [60]PCBM due to their higher LUMO energy levels, and the absorption spectra of these compounds also have better overlap with the solar spectrum. Moreover, they have higher electron carrier mobilities comparing with [60]PCBM. We suggest that the better photophysical and charge transport properties of this new generation of H-shaped compounds with strain and Hückel aromaticity based on 99′**BF** backbone can be promising organic semiconductor for HJOPVs.

In addition, further investigations into the photovoltaic properties of another nonfullerene small-molecule acceptor materials for HJOPVs as well as the reasonable design of other members of this class of D-A-D systems are now underway and will be reported in future publications.

Acknowledgments We gratefully acknowledge the financial support from the National Natural Science Foundation of China (Project No. 20903020), National Basic Research Program of China (973 Program-2009CB623605), the Science and Technology Development Project Foundation of Jilin Province (20090146), and the Science and Technology Development Planning of Yan Bian University (201103).

References

1. Jung JW, Lee JU, Jo WH (2010) J Phys Chem C 114:633. doi:10.1021/jp9083844
2. Ferry VE, Munday JN, Atwater HA (2010) Adv Mater 22:4794. doi:10.1002/adma.201000488
3. Nelson J, Kwiatkowski JJ, Kirkpatrick J, Frost JM (2009) Acc Chem Res 42:1768. doi:10.1021/ar900119f
4. Cheng YJ, Yang SH, Hsu CS (2009) Chem Rev 109:5868. doi:10.1021/cr900182s
5. Gommans H, Aernouts T, Verreet B, Heremans P, Medina A, Claessens CG, Torres T (2009) Adv Funct Mater 19:3435. doi:10.1002/adfm.200900524
6. Heremans P, Cheyns D, Rand BP (2009) Acc Chem Res 42:1740. doi:10.1021/ar9000923
7. Debucquoy M, Rockele M, Genoe J, Gelinck GH, Heremans P (2009) Org Electron 10:1252. doi:10.1016/j.orgel.2009.07.005
8. Lee MR, Eckert RD, Forberich K, Dennler G, Brabec CJ, Gaudiana RA (2009) Science 324:232. doi:10.1126/science.1168539
9. Dennler G, Scharber MC, Brabec CJ (2009) Adv Mater 21:1323. doi:10.1002/adma.200801283
10. Günes S, Neugebauer H, Sariciftci NS (2007) Chem Rev 107:1324. doi:10.1021/cr050149z
11. Scharber MC, Mühlbacher D, Koppe M, Denk P, Waldauf C, Heeger AJ, Brabec CJ (2006) Adv Mater 18:789. doi:10.1002/adma.200501717
12. Koster LJA, Mihailetchi VD, Blom PWM (2006) Appl Phys Lett 88:093511. doi:10.1063/1.2181635
13. Peet J, Kim JY, Coates NE, Ma WL, Moses D, Heeger AJ, Bazan GC (2007) Nat Mater 6:497. doi:10.1038/nmat1928
14. Thompson BC, Fréchet JMJ (2008) Angew Chem Int Ed 47:58. doi:10.1002/anie.200702506
15. Blouin N, Michaud A, Gendron D, Wakim S, Blair E, Neagu-Plesu R, Belletête M, Durocher G, Tao Y, Leclerc M (2008) J Am Chem Soc 130:732. doi:10.1021/ja0771989
16. Blouin N, Michaud A, Leclerc M (2007) Adv Mater 19:2295. doi:10.1002/adma.200602496
17. Park SH, Roy A, BeaupréS ChoS, Coates N, Moon JS, Moses D, Leclerc M, Lee K, Heeger AJ (2009) Nat Photonics 3:297. doi:10.1038/nphoton.2009.69
18. Granström M, Petritsch K, Arias AC, Lux A, Andersson MR, Friend RH (1998) Nature 395:257. doi:10.1038/26183
19. Koetse MM, Sweelssen J, Hoekerd KT, Schoo HFM, Veenstra SC, Kroon JM, Yang X, Loos J (2006) Appl Phys Lett 88:083504. doi:10.1063/1.2176863
20. Zhan X, Tan Za, Domercq B, An Z, Zhang X, Barlow S, Li Y, Zhu D, Kippelen B, Marder SR (2007) J Am Chem Soc 129:7246. doi:10.1021/ja071760d
21. Miller EK, Lee K, Hasharoni K, Hummelen JC, Wudl F, Heeger AJ (1998) J Chem Phys 108:1390. doi:10.1063/1.475550
22. Hummelen JC, Knight BW, Lepeq F, Wudl F, Yao J, Wilkins CL (1995) J Org Chem 60:532. doi:10.1021/jo00108a012
23. Yu G, Gao J, Hummelen JC, Wudl F, Heeger AJ (1995) Science 270:1789. doi:10.1126/science.270.5243.1789
24. Yang C, Cho S, Heeger AJ, Wudl F (2009) Angew Chem Int Ed 48:1592. doi:10.1002/anie.200805228
25. Wienk MM, Turbiez M, Gilot J, Janssen RAJ (2008) Adv Mater 20:2556. doi:10.1002/adma.200800456
26. Backer SA, Sivula K, Kavulak DF, Fréchet JMJ (2007) Chem Mater 19:2927. doi:10.1021/cm070893v
27. Lenes M, Shelton SW, Sieval AB, Kronholm DF, Hummelen JC, Blom PWM (2009) Adv Funct Mater 19:3002. doi:10.1002/adfm.200900459
28. Lenes M, Wetzelaer G, Kooistra FB, Veenstra SC, Hummelen JC, Blom PWM (2008) Adv Mater 20:2116. doi:10.1002/adma.200702438
29. Diederich F, Kessinger R (1999) Acc Chem Res 32:537. doi:10.1021/ar970321o
30. Matsumoto K, Hashimoto K, Kamo M, Uetani Y, Hayase S, Kawatsura M, Itoh TJ (2010) Mater Chem 20:9226. doi:10.1039/C0JM01565B
31. Chen CP, Chan SH, Chao TC, Ting C, Ko BT (2008) J Am Chem Soc 130:12828. doi:10.1021/ja801877k

32. Cremer J, Bäuerle PJ (2006) J Mater Chem 16:874. doi:10.1039/b515657b
33. Cravino A, Leriche P, Aleveque O, Roquet S, Roncali J (2006) Adv Mater 18:3033. doi:10.1002/adma.200601230
34. Luo J, Zhao BM, Chan HSO, Chi CY (2010) J Mater Chem 20:1932. doi:10.1039/b918671a
35. Luo J, Zhao BM, Shao JJ, Lim KA, Chan HSO, Chi CY (2009) J Mater Chem 19:8327. doi:10.1039/b913930c
36. Sun XB, Liu YQ, Chen SY, Qiu WF, Yu G, Ma YQ, Qi T, Zhang HJ, Xu XJ, Zhu DB (2006) Adv Funct Mater 16:917. doi:10.1002/adfm.200500463
37. Zen A, Bilge A, Galbrecht F, Alle R, Meerholz K, Grenzer J, Neher D, Scherf U, Farrell T (2006) J Am Chem Soc 128:3914. doi:10.1021/ja0573357
38. Bilge A, Zen A, Forster M, Li HB, Galbrecht F, Nehls BS, Farrell T, Neher D, Scherf U (2006) J Mater Chem 16:3177. doi:10.1039/b605338f
39. Benincori T, Capaccio M, De Angelis F, Falciola L, Muccini M, Mussini P, Ponti A, Toffanin S, Traldi P, Sannicolo F (2008) Chem Eur J 14:459. doi:10.1002/chem.200701117
40. Ohmae T, Nishinaga T, Wu M, Iyoda M (2010) J Am Chem Soc 132:1066. doi:10.1021/ja908161r
41. Mitchell WJ, Ferguson AJ, Kose ME, Rupert BL, Ginley DS, Rumbles G, Shaheen SE, Kopidakis N (2009) Chem Mater 21:287. doi:10.1021/cm802410d
42. Rupert BL, Mitchell WJ, Ferguson AJ, Kose ME, Rance WL, Rumbles G, Ginley DS, Shaheen SE, Kopidakis NJ (2009) Mater Chem 19:5311. doi:10.1039/b903427g
43. Ma CQ, Fonrodona M, Schikora MC, Wienk MM, Janssen RAJ, Bauerle P (2008) Adv Funct Mater 18:3323. doi:10.1002/adfm.200800584
44. Brunetti FG, Gong X, Tong M, Heeger AJ, Wudl F (2010) Angew Chem Int Ed 49:532. doi:10.1002/anie.200905117
45. Marcus RA (1956) J Chem Phys 24:966. doi:10.1063/1.1742723
46. Marcus RA (1993) Rev Mod Phys 65:599. doi:10.1103/RevModPhys.65.599
47. Marcus RA, Sutin N (1985) Biochim Biophys Acta 811:265. doi:10.1016/0304-4173(85)90014-X
48. Troisi A, Orlandi G (2006) J Phys Chem A 110:4065. doi:10.1021/jp055432g
49. Hush NS (1961) Trans Faraday Soc 57:557. doi:10.1039/TF9615700557
50. Jortner J (1976) J Chem Phys 64:4860. doi:10.1063/1.432142
51. Yang X, Li Q, Shuai Z (2007) Nanotechnology 18:424029. doi:10.1088/0957-4484/18/42/424029
52. Yang X, Wang L, Wang C, Long W, Shuai Z (2008) Chem Mater 20:3205. doi:10.1021/cm8002172
53. Gao H, Qin C, Zhang H, Wu S, Su ZM, Wang Y (2008) J Phys Chem A 112:9097. doi:10.1021/jp804308e
54. Hutchison GR, Ratner MA, Marks TJ (2005) J Am Chem Soc 127:16866. doi:10.1021/ja0533996
55. Troisi A, Orlandi G (2001) Chem Phys Lett 344:509. doi:10.1016/S0009-2614(01)00792-8
56. Yin S, Yi Y, Li Q, Yu G, Liu Y, Shuai Z (2006) J Phys Chem A 110:7138. doi:10.1021/jp057291o
57. Valeev EF, Coropceanu V, Da Silva Filho DA, Salman S, Brédas JL (2006) J Am Chem Soc 128:9882. doi:10.1021/ja061827h
58. Siders P, Marcus RA (1981) J Am Chem Soc 103:748. doi:10.1021/ja00394a004
59. Brunschwig BS, Logan J, Newton MD, Sutin N (1980) J Am Chem Soc 102:5798. doi:10.1021/ja00538a017
60. Hutchison GR, Ratner MA, Marks TJ (2005) J Am Chem Soc 127:2339. doi:10.1021/ja0461421
61. Frisch M, Trucks GW.; Schlegel HB, Scuseria GE, Robb MA, CheesemanJR, Scalmani G, Barone V, Mennucci BG, Petersson A, Nakatsuji H, Caricato M, Li X, Hratchian HP, Izmaylov AF, Bloino J, Zheng G, Sonnenberg JL, Hada M, Ehara M, Toyota K, Fukuda R, Hasegawa J, Ishida M, Nakajima T, Honda Y, Kitao O, Nakai H, Vreven T, Montgomery JA Jr, Peralta JE, Ogliaro F, Bearpark M, Heyd JJ, Brothers E, Kudin KN, Staroverov VN, Kobayashi R, Normand J, Raghavachari K, Rendell A, Burant JC, Iyengar SS, Tomasi J, Cossi M, Rega N, Millam JM, Klene M, Knox JE, Cross JB, Bakken V, Adamo C, Jaramillo J, Gomperts R, Stratmann RE, Yazyev O, Austin AJ, Cammi R, Pomelli C, Ochterski JW, Martin RL, Morokuma K, Zakrzewski VG, Voth GA, Salvador P, Dannenberg JJ, Dapprich S, Daniels AD, Farkas O, Foresman JB, Ortiz JV, Cioslowski J, Fox DJ (2009) Gaussian 09, Revision A.02. Gaussian, Inc., Wallingford
62. Lee CT, Yang WT, Parr RG (1988) Phys Rev B 37:785. doi:10.1103/PhysRevB.37.785
63. Song Y, Di Ca, Yang X, Li S, Xu W, Liu Y, Yang L, Shuai Z, Zhang D, Zhu D (2006) J Am Chem Soc 128:15940. doi:10.1021/ja064726s
64. Lee JS, Nyburg SC (1985) Acta Crystallogr Sect C Cryst Struct Commun 41:560. doi:10.1107/S010827018500467X
65. Sonar P, Fong Lim JP, Chan KL (2011) Energy Environ Sci 4:1558. doi:10.1039/C0EE00668H
66. Service RF (2011) Science 332:293. doi:10.1126/science.332.6027.293
67. Liao Y, Yang GC, Feng JK, Shi LL, Yang SY, Yang L, Ren AM (2006) J Phys Chem A 110:13036. doi:10.1021/jp061326i
68. Gong X, Tong MH, Brunetti FG, Seo J, Sun YM, Moses D, Wudl F, Heeger AJ (2011) Adv Mater 23:2272. doi:10.1002/adma.201003768
69. Sadlej AJ (1988) Collect Czech Chem Commun 53:1995. doi:10.1135/cccc19881995
70. Mihailetchi VD, Van Duren JKJ, Blom PWM, Hummelen JC, Janssen RAJ, Kroon JM, Rispens MT, Verhees WJH, Wienk MM (2003) Adv Funct Mater 13:43. doi:10.1002/adfm.200390004